

^4He abundances: Optical versus radio recombination line measurements

Dana S. Balsa¹, Robert T. Rood² and T. M. Bania³

¹National Radio Astronomy Observatory, 520 Edgemont Road, Charlottesville, VA 22903-2475 USA
email: dbalser@nrao.edu

² Astronomy Department, University of Virginia, P.O.Box 3818, Charlottesville VA 22903-0818, USA
email: rtr@virginia.edu

³ Institute for Astrophysical Research, 725 Commonwealth Avenue, Boston University, Boston MA 02215, USA
email: bania@bu.edu

Abstract. Accurate measurements of the $^4\text{He}/\text{H}$ abundance ratio are important in constraining Big Bang nucleosynthesis, models of stellar and Galactic evolution, and H II region physics. We discuss observations of radio recombination lines using the Green Bank Telescope toward a small sample of H II regions and planetary nebulae. We report $^4\text{He}/\text{H}$ abundance ratio differences as high as 15 – 20% between optical and radio data that are difficult to reconcile. Using the H II regions S206 and M17 we determine ^4He production in the Galaxy to be $dY/dZ = 1.71 \pm 0.86$.

Keywords. Galaxy: abundances, ISM: planetary nebulae, H II regions, radio lines: ISM

1. Introduction

Observations of optical recombination lines (ORLs) are the primary diagnostics used to determine ^4He abundances in ionized nebulae such as H II regions and planetary nebulae (PNe). At optical wavelengths there are also many bright collisionally excited lines that can be used to probe the physical conditions in these objects and to derive their metallicity. Peimbert *et al.* (2010) discuss the main uncertainties in calculating accurate $^4\text{He}/\text{H}$ abundance ratios from ORLs. Much of the focus has been on deriving ^4He abundances in metal poor objects, such as blue compact galaxies, to deduce the primordial $^4\text{He}/\text{H}$ abundance (e.g., see Izotov 2010; Skillman 2010). Because there is no way to directly measure neutral helium within the H II region it is difficult to determine accurate $^4\text{He}/\text{H}$ abundance ratios for most Galactic H II regions due to the relatively soft ionizing radiation field for most objects. One exception is M17 which contains several O3 type stars and is estimated to contain little neutral helium (e.g., Carigi & Peimbert 2008).

Observations of recombination lines at other wavelengths (e.g., radio and infrared) give important checks to ORLs since deriving $^4\text{He}/\text{H}$ abundance ratios using these transitions will have different systematic uncertainties. Moreover, recombination lines at radio and infrared wavelengths are not obscured by dust and may be used to probe ^4He abundances throughout the Galactic disk.

Radio recombination lines (RRLs) are relatively weak when compared to ORLs and emission measures of $\int n_e^2 d\ell \sim 10^3 \text{ cm}^{-6} \text{ pc}$ are required to detect these lines with current instrumentation compared with $\sim 1 \text{ cm}^{-6} \text{ pc}$ at optical wavelengths. Recent improvements in radio spectrometers, however, now allow the simultaneous observation of multiple RRLs. Adjacent RRLs have line intensities and widths that are different by

only a few percent. Therefore, averaging adjacent RRLs can be used to increase the signal-to-noise ratio without significantly increasing the error in the line parameters.

Besides sensitivity, the main problem in making accurate ^4He measurements using RRLs has been poor spectral baselines. For single-dish telescopes reflections from the super-structure cause standing waves that are not easy to model and that do not integrate down with time. (Although the spectral baselines are much better for radio interferometers, until recently the spectral resolution and bandwidth were not sufficient to produce accurate line parameters in most cases.) The off-axis, clear aperture design of the Green Bank Telescope (GBT) has significantly improved the spectral baselines, and when combined with a flexible spectrometer provides a significant improvement over previous telescopes when measuring weak, wide spectral lines (e.g., Balser 2006; Bania *et al.* 2010).

One advantage to using RRLs over ORLs is that the high n states of hydrogen and helium should be altered by radiative and collisional effects in the same way so that the ratio of the line areas is equal to the ionic abundance ratio. At high n , where the levels are controlled by collisions and are in LTE, this should certainly be the case. H II region models indicate that near $n \sim 90$ (9 GHz) the RRLs are approximately in LTE (Shaver 1980; Balser *et al.* 1999). Early RRL observations of Galactic H II regions, however, produced $^4\text{He}^+/\text{H}^+$ abundance ratios that varied with n (Lockman & Brown 1982). Peimbert *et al.* (1992) studied α , β , and γ RRL transitions near 9 GHz with the same spatial resolution and derived $^4\text{He}^+/\text{H}^+$ abundance ratios consistent within the errors. These data had better sensitivity and improved spectral baselines over previous RRL measurements (Balser *et al.* 1994).

Ionization and density structure must be understood when using either optical or radio recombination lines to calculate $^4\text{He}/\text{H}$ abundance ratios. Since there is no transition of neutral helium other diagnostics must be used to determine if any neutral helium resides within the H II region. Therefore, corrections for ionization structure often contribute significantly to the uncertainty in calculating the $^4\text{He}/\text{H}$ abundance ratio (e.g., Baldwin *et al.* 1991). This is why H II regions with very hard radiation fields are often chosen for ^4He studies (e.g., blue compact galaxies). Nevertheless, a reverse ionization correction can result in these objects wherein neutral hydrogen exists within the He II region (Ballantyne *et al.* 2000; Gruenwald *et al.* 2002; Sauer & Jedamzik 2002). Moreover, when combined with density structures the ionization correction factor will change (Viegas *et al.* 2000). Also, density structure alone can alter the radiative transfer and thus effect ^4He analyses (Mathis & Wood 2005).

2. Observations

We made GBT RRL observations toward four PNe (NGC 3242, NGC 6826, NGC 6543, and NGC 7009) and two Galactic H II regions (M17 and S206). All observations were made at X-band (8 – 10 GHz) with a spatial resolution (beam) of 80 arcsec and a spectral resolution of 0.4 km s^{-1} . The PNe observations were part of the ^3He experiment wherein the 91α and 92α H and He RRLs were observed simultaneously with the $^3\text{He}^+$ hyperfine transition (see Bania *et al.* 2010). These PNe consist of multiple shells with large, extended halos. The RRL emission arises from the shell structure which is unresolved by the GBT beam. Because the hot central star produces a hard ionizing radiation field there should be little or no neutral helium in these nebulae.

The H II region observations were part of a Galactic H II survey measuring H, He and C RRL emission. Seven adjacent alpha RRLs were observed simultaneously ($87\alpha - 93\alpha$). M17 and S206 are expected to have little neutral helium and therefore are good candidates

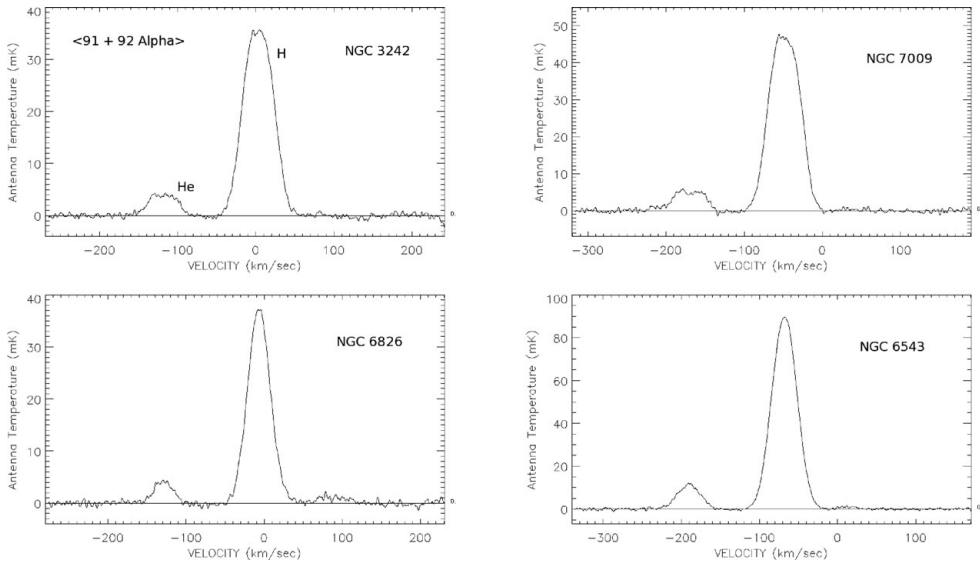


Figure 1. Planetary nebulae GBT RRL spectra. Plotted is the antenna temperature in mK versus the LSR velocity in km s^{-1} . The 91α and 92α RRLs have been averaged and the spectra smoothed to a velocity resolution of 2.0 km s^{-1} . The continuum emission has been subtracted.

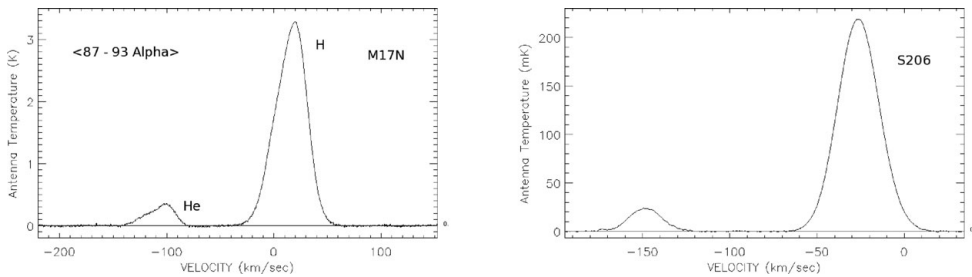


Figure 2. H II region GBT RRL spectra. Plotted is the antenna temperature in mK versus the LSR velocity in km s^{-1} . RRLs spanning 87α to 93α have been averaged. The continuum emission has been subtracted.

for measuring $^4\text{He}/\text{H}$ (e.g., Deharveng *et al.* 2000; Carigi & Peimbert 2008). Both M17 and S206 are extended relative to the GBT beam and thus we are only probing part of these nebulae. Results for S206 have already been published (Balsler 2006). The M17 data consist of observations toward a northern (M17N) and a southern (M17S) component. Since M17S is optically obscured, we discuss M17N here to make comparisons with ORLs. Our M17N J2000 position (RA = 18:17:46.5, Dec = $-16:10:33.1$) overlaps with some optical positions.

The PNe spectra are summarized in Figure 1. The H and ^4He line profiles for NGC 3242 and NGC 7009 are square-shaped, consistent with an optically thin, unresolved, expanding nebulae. When the expansion velocity is small compared with the thermal and turbulent velocity dispersion then the line profiles will become Gaussian shaped. This appears to be the case for NGC 6826 and NGC 6543 since the line profiles for these objects are well modeled by a Gaussian function.

The H II region spectra are summarized in Figure 2. The line profiles are well fit by Gaussian components. M17N is best fit by two components and S206 by one component.

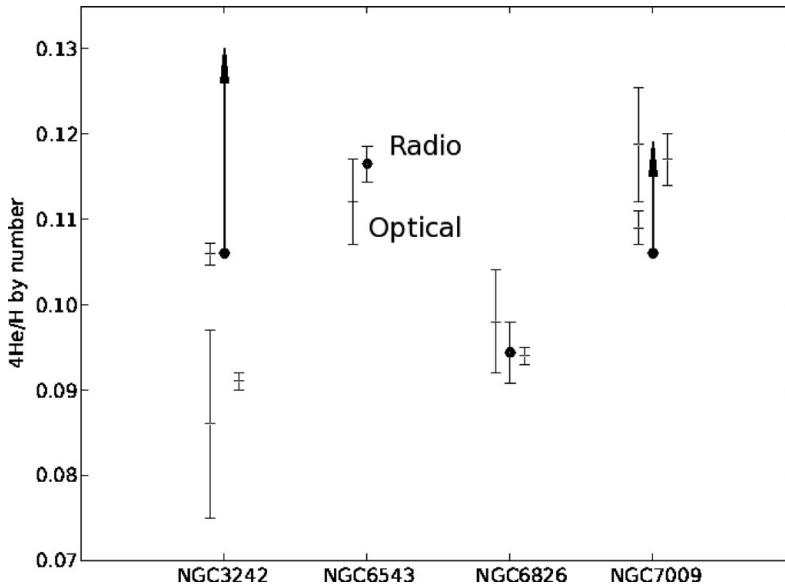


Figure 3. $^4\text{He}/\text{H}$ abundance ratios by number for the planetary nebulae sample. Filled circles are GBT results, while the plus sign symbols are from ORLs in the literature (Barker 1983, 1985, 1988; Perinotto *et al.* 2004; Krabbe & Copetti 2006).

In both nebulae carbon RRL emission is detected. The signal-to-noise ratio is excellent and the spectral baselines well behaved.

3. Results and discussion

The ^4He abundances for our PNe sample are shown in Figure 3. The GBT $^4\text{He}/\text{H}$ abundance ratios are calculated assuming $^4\text{He}/\text{H} = ^4\text{He}^+/\text{H}^+$. For NGC 3242 and NGC 7009 $^4\text{He}^{++}$ has been detected and thus our abundance estimates are only limits as indicated by the arrows in Figure 3. The tip of the arrow is an estimate of $^4\text{He}/\text{H}$ using the $^4\text{He}^{++}/^4\text{He}^+$ ratios from Cahn *et al.* (1992) and assuming a uniform distribution of $^4\text{He}^+$ and $^4\text{He}^{++}$. The optical and radio data are in excellent agreement except for NGC 3242. This PN has significant amounts of $^4\text{He}^{++}$, however, that may not be distributed uniformly. Therefore, the estimate of $^4\text{He}/\text{H}$ for the GBT data shown in Figure 3 may be smaller than indicated.

Figure 4 shows the derived abundance by mass, Y , plotted as a function of nebular metallicity, Z . Both Galactic and extragalactic H II region ^4He abundances are plotted as symbols together with an estimate of ^4He processing, dY/dZ , shown by the solid lines. For the GBT H II region data we again assume $^4\text{He}/\text{H} = ^4\text{He}^+/\text{H}^+$. The optical data shown for M17 are based on two different positions: M17-14 and M17-123 (an average of M17-1, M17-2, and M17-3) (Peimbert *et al.* 1992). The high ^4He optical value shown in Figure 4 is from M17-123 and is expected to be a better estimate of $^4\text{He}/\text{H}$ since this region has a higher degree of ionization and therefore less neutral helium (Carigi & Peimbert 2008). Although the radio ^4He abundance is the same within the errors as the optical value for position M17-14, the GBT position overlaps with position M17-3 and not with M17-14. Yet the GBT $^4\text{He}/\text{H}$ abundance ratio is significantly smaller than the optical value for position M17-3. This discrepancy may result because the large GBT beam averages over regions with different properties.

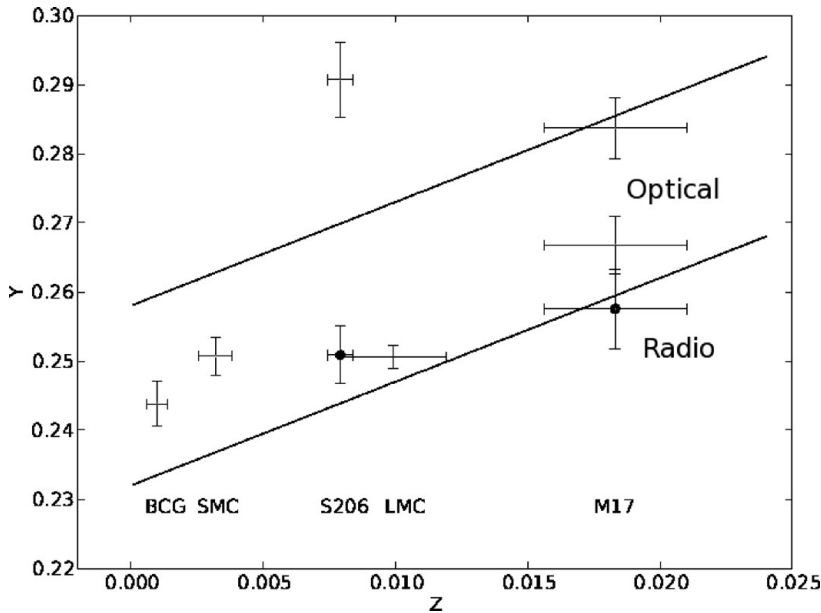


Figure 4. Evolution of $^4\text{He}/\text{H}$. The helium abundance by mass, Y , is plotted against the metallicity, Z . GBT results are shown as filled circles for M17 and S206 while ORL results are plus signs for M17 (Carigi & Peimbert 2008; García-Rojas *et al.* 2007), the Small Magellanic Cloud (Peimbert *et al.* 2007), the Large Magellanic Cloud (Peimbert 2003), and a sample of blue compact galaxies (Izotov & Thuan 2004). The solid lines assume the range of primordial $^4\text{He}/\text{H}$ abundance ratios from Olive & Skillman (2004) and $dY/dZ = 1.5$ (Chiappini *et al.* 2002).

The ^4He abundances for S206 are puzzling. Deharveng *et al.* (2000) measure no variation in $^4\text{He}/\text{H}$ across S206 and values of O^{++}/O that range from 0.7 to 0.85; they conclude that there is no neutral helium in the nebula. S206 is ionized primarily by an O5 type star—the nebula structure is simple compared with M17 and contains less dust. Therefore, S206 should be an excellent candidate for measuring $^4\text{He}/\text{H}$.

But the optical value for $^4\text{He}/\text{H}$ is 20% higher than the radio value. This discrepancy is difficult to reconcile and the optical result is not consistent with our understanding of Galactic chemical evolution. We expect there to be a net production of ^4He in stars and therefore $dY/dZ > 0$. This is illustrated by the two solid lines in Figure 4 where we have adopted the ^4He Galactic production of $dY/dZ = 1.5$ from Chiappini *et al.* (2002) and the conservative range for the ^4He primordial abundance from Olive & Skillman (2004). For the Milky Way we derive $dY/dZ = 1.71 \pm 0.86$ by using only the radio $^4\text{He}/\text{H}$ value for S206, both the optical and radio $^4\text{He}/\text{H}$ values for M17, and the primordial $^4\text{He}/\text{H}$ abundance ratio from Steigman (2007).

References

- Baldwin, J. A., Ferland, G. J., Martin, P. G., Corbin, M. R., Cota, S. A., Peterson, B. M., & Slettebak, A. 1991, *ApJ*, 374, 580
- Ballantyne, D. R., Ferland, G. J., & Martin, P. G. 2000, *ApJ*, 536, 773
- Balser, D. S. 2006, *AJ*, 132, 2326
- Balser, D. S., Bania, T. M., Brockway, C. J., Rood, R. T., & Wilson, T. L. 1994, *ApJ*, 430, 667
- Balser, D. S., Bania, T. M., Rood, R. T., & Wilson, T. L. 1999, *ApJ*, 510, 759

- Bania, T. M., Rood, R. T., & Balsler, D. S. 2010, in: *Light Elements in the Universe* C. Charbonnel, M. Tosi, F. Primas, & C. Chiappini (eds.), Proc. IAU Symposium No. 268, (Cambridge: CUP), p. XX
- Barker, T. 1983, *ApJ*, 267, 630
- Barker, T. 1985, *ApJ*, 294, 193
- Barker, T. 1988, *ApJ*, 326, 164
- Cahn, J. H., Kaler, J. B., & Stanghellini, L. 1992, *A&AS*, 94, 399
- Carigi, L. & Peimbert, M. 2008, *Rev. Mexicana AyA*, 44, 311
- Chiappini, C., Renda, A., & Matteucci, F. 2002, *A&A*, 395, 789
- Deharveng, L., Peña, M., Caplan, J., & Costero, R. 2000, *MNRAS*, 311, 329
- García-Rojas, J., Esteban, C., Peimbert, A., Rodríguez, M., Peimbert, M., & Ruiz, M. T. 2007, *Rev. Mexicana AyA*, 43, 3
- Gruenwald, R., Steigman, G., & Viegas, S. M. 2002, *ApJ*, 567, 931
- Izotov, Y. I. 2010, in: *Light Elements in the Universe* C. Charbonnel, M. Tosi, F. Primas, & C. Chiappini (eds.), Proc. IAU Symposium No. 268, (Cambridge: CUP), p. XX
- Izotov, Y. I. & Thuan, T. X. 2004, *ApJ*, 602, 200
- Krabbe, A. C. & Copetti, M. V. F. 2006, *A&A*, 450, 159
- Lockman, F. J. & Brown, R. L. 1982, *ApJ*, 259, 595
- Mathis, J. S. & Wood, K. 2005, *MNRAS*, 360, 227
- Peimbert, A. 2003, *ApJ*, 584, 735
- Peimbert, M., Luridiana, V., & Peimbert, A. 2007, *ApJ*, 666, 636
- Peimbert, P., Peimbert, A., Carigi, L., & Luridiana, V. 2010, in: *Light Elements in the Universe* C. Charbonnel, M. Tosi, F. Primas, & C. Chiappini (eds.), Proc. IAU Symposium No. 268, (Cambridge: CUP), p. XX volume
- Peimbert, M., Rodríguez, L. F., Bania, T. M., Rood, R. T., & Wilson, T. L. 1992a, *ApJ*, 395, 484
- Peimbert, M., Torres-Peimbert, S., & Ruiz, M. T. 1992b, *Rev. Mexicana AyA*, 24, 155
- Perinotto, M., Morbidelli, L., & Scatarzi, A. 2004, *MNRAS*, 349, 793
- Olive, K. A. & Skillman, E. D. 2004, *ApJ*, 617, 29
- Sauer, D. & Jedamizik, K. 2002, *A&A*, 381, 361
- Shaver, P. A. 1980, *A&A*, 91, 279
- Skillman, E. 2010, in: *Light Elements in the Universe* C. Charbonnel, M. Tosi, F. Primas, & C. Chiappini (eds.), Proc. IAU Symposium No. 268, (Cambridge: CUP), p. XX
- Steigman, G. 2007, *Ann. Rev. Nucl. Part. Sci.*, 57, 463
- Viegas, S. M., Gruenwald, R., & Steigman, G. 2002, *ApJ*, 531, 813